ORIGINAL PAPER

Seismic risk assessment as part of the National Risk Assessment for the Republic of Cyprus: from probabilistic to scenario-based approach

Danai Kazantzidou-Firtinidou[1] · Nicholas Kyriakides[2] · Renos Votsis[2] · Christis Z. Chrysostomou[2]

Abstract

Seismic risk assessment for Cyprus at national scale is based on event-based probabilistic seismic risk analysis and eventual selection of seismic scenarios for given return periods. The current study was included in the National Risk Assessment of Cyprus, for 2018, following the European Commission requirements and guidelines. The latter analysis is performed with the relevant algorithm of Open Quake engine, which first incorporates stochastic event-based hazard analysis for extended earthquake catalogues and models of the area, as developed in the ESHM13 model developed in the SHARE project. The exposure model employed is built and elaborated by local resources, and the vulnerability model developed for local building typologies, as included in past publications, was used, with additional considerations. Risk is expressed in terms of monetary loss, at national level and for the biggest urban areas, and is provided in aggregated values as well as distributed along the island with map representation. For the selected scenarios, with 475- and 2500-year return period, expected casualties and displaced population are also estimated.

Keywords Cyprus · Seismic risk · Disaster risk reduction · Probabilistic risk analysis · Seismic scenario

1 Introduction

Following the decision of the European Parliament and of the Council (1313/2013/EU), the Member States are required to submit a summary of National Risk assessment (NRA) to the Union Civil Protection Mechanism. At the end of 2018, the Republic of

---

✉ Nicholas Kyriakides
  nicholas.kyriakides@cut.ac.cy

  Danai Kazantzidou-Firtinidou
  d.kazantzidou@kemea-research.gr

1 Center for Security Studies (KEMEA), Ministry of Citizen Protection, Athens, Greece

2 Department of Civil Engineering and Geomatics, Cyprus University of Technology, Limassol, Cyprus

Cyprus was committed to submit the 3rd version of NRA, responding to a twofold target: produce a NRA that complies with EU guidelines, allowing for comparison with other member states, and provide all necessary information based on a quantitative approach for risk metric estimate, supporting efforts for targeted disaster management planning. As a matter of fact, the peer review (ECORYS & Fraunhofer 2018), conducted on behalf of the Commission, on civil protection and disaster risk management, recommended the use of NRA outcomes for prevention and mitigation actions at states authorities level, as well as public risk awareness.

Understanding risk is the first priority action of the Sendai Framework (UNISDR 2015). Policies and measures are recommended to be based on risk-driven results, accounting for uncertainties, yet with scientific and multidisciplinary estimates. For effective disaster risk management, it is crucial to analyse and have an understanding of multiple hazards and their linkages with vulnerabilities, contributing to risk levels of different types. Moreover, the latest GAR (UNDRR 2019) underlines that risk can no longer be considered and addressed individually, and its systemic nature should rather be understood and studied, acknowledging all social, economic, political and ecological dimensions. Hence, NRA methodology is based on multidimensional components, as proposed by UNISDR (2017) guidelines. This implies the selection of hazards, the impact assessment at different levels (direct and indirect) and the overall risk estimate. For Cyprus NRA, Cyprus Civil Defence Agency selected the hazards to be included in the study. For each hazard, according to its nature, available input and loss data, different risk analysis methodologies have been implemented, varying from qualitative and experts' elicitation to probabilistic quantitative analysie.

Earthquakes have been recognized as one of the main hazards affecting Cyprus, as already included into the National Risk Assessment implemented by Cyprus Civil Defence in 2016 (CCDD 2016). According to historical records (Ambraseys 1965; Galanopoulos and Delibasis 1965; Kalogeras et al. 1999), Cyprus has suffered from at least 16 destructive earthquakes in the past 2000 years and numerous smaller earthquakes. The largest earthquakes mostly occurred at the southern part of the island, causing damage in Paphos, Limassol and Famagusta (Cagnan and Tanircan 2010). The latest deadliest earthquake that hit the island was in 1953 (M_w6.1) with an aftermath of 40 fatalities, 100 injuries and extensive damage to 158 villages and the city of Paphos (Ambraseys 1992). According to the disaster risk profile of Cyprus (ECORYS & Fraunhofer 2018), based on historical data, earthquake is the natural disaster with the second most important monetary impact and the first in terms of population affected.

The risk assessment process, as documented by EC (2010), UNISDR (2017) Guidelines and ISO 31000 (2018) and ISO31010 (2019), has been followed. This is composed by the steps of *risk identification*, *risk analysis* and *risk evaluation*. *Risk identification* includes the identification of causes of risk, *i.e.* hazard and circumstances, the definition of the area of study, exposed assets and different risk metrics. For the study of seismic risk assessment, hazard definition corresponds to the selection of the most valuable earthquake scenarios, the collection of data on buildings and population at national level and the selection of the most appropriate impact metrics. *Risk analysis* is the fundamental step of risk assessment and is the "the combination of the consequences of an event or hazard and the associated likelihood of its occurrence" (ISO 2019). Probabilistic risk analysis has been performed to estimate consequences with given probabilities of occurrence, while it allows for selection of seismic scenarios with return periods frequently used in disaster planning. Scenario-based analysis simulates the "way the future may develop" (EC 2010) and provides comprehensive and understandable results at different

terms to risk management stakeholders. *Risk evaluation* is the step that allows for prioritization of risks for the purposes of risk management. Herein, it has been implemented with empirical criteria for the establishment of overall risk matrices.

For the performance of seismic hazard and risk analysis, the OpenQuake engine (Silva et al. 2013), developed within the Global Earthquake Model Foundation (GEM 2020a, b), has been applied. The engine is open-source and has the possibility to perform both probabilistic hazard and risk assessment and scenario damage and risk computation. Tailor-made hazard, exposure and vulnerability models have been uploaded together with customized logic trees to account for epistemic uncertainties. Data granted by past scientific projects and local stakeholders have been implemented after appropriate elaboration. The open-source QGIS software has been used for mapping of the results.

2 Seismic hazard of Cyprus

Cyprus is located at the boundary between the Eurasian, Arabian and African plates within a complex tectonic setting (e.g. Papazachos and Papaioannou 1999). Cyprus Arc accommodates the movement between the African and Anatolian subplate and, although less active than the Hellenic Arc, it has been the origin of several shallow earthquakes (Fig. 1) mostly of medium size. It is worth noticing that the first seismometer was installed in the island in 1984, while modern instrumentation began in the island only after 1997 after the M_w6.8 earthquake at the onshore area of Pafos in 1996. Until then, the seismic catalogue was composed by historical empirical relationships and various international sources.

Cyprus tectonic regime has been for long a field for debate for seismologists. Cyprus seismic activity is due to its location at two seismogenic tectonic regions. On the one hand, there is the subduction of the African plate moving northwards under the Anatolian subplate moving westwards, and on the other hand there is the major continental collision of the Eurasian plate with the African one. Cyprus Arc itself is subdivided into three regions of different seismicity: its north-western part, connected to the Hellenic Arc, being the most active with earthquakes of intermedium depth (60–130 km); the central-south-western one, almost parallel to the south-south-western shores of the island and the eastern
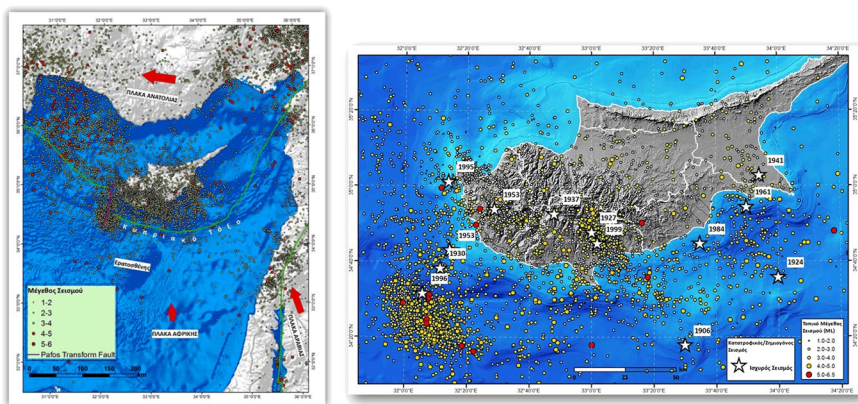

Fig. 1 Seismic activity in Cyprus between 1896 and 2018 (CGSD 2017)

one, characterized by multiple and surface earthquakes. The variations of the seismic activity of the two western sections (in depth and magnitude) indicate that the north-western section consists of a subduction boundary, while the south-western one a collision zone (Wdowinski et al. 2006). The two sections are separated by the NE–SW strike–slip Paphos fault, able to produce large earthquakes, as the M_w6.8 1996 Paphos earthquake. The eastern section is extended until the triple contact point of the Arabian, African and Eurasian plat is oriented almost parallel to the plates motion and is characterized by low seismicity and transcurrent tectonic activity. Furthermore, neotectonic onshore faults on the crust are additional seismogenic sources, although no thorough study has been conducted on them (Cagnan and Tanircan 2010).

In the current study, while expecting ESHM20 (ongoing under H2020 SERA project-GA 730,900), the updated seismic hazard model for Europe, the available ESHM13 consistent seismic hazard model for Europe and Turkey developed in the SHARE project (Giardini et al. 2013) has been used, herein. Input hazard models have been prepared in the OpenQuake format (Pagani et al. 2014) in order to provide a regional input to "Global Earthquake Model" initiative. A number of existing databases, as explained below, have been incorporated into the hazard models, taking into account the epistemic uncertainties of the model components and hazard results.

More precisely, the seismicity of Cyprus was input into the SHARE European Earthquake Catalogue (Stucchi et al. 2013) as part of the SHARE earthquake catalogue compiled by Sesetyan et al. (2011). The latter was compiled within SHARE and EMME (Erdik et al. 2012) project and included the seismic catalogue between 1000 and 2006, with a total of 6170 events. The classic area source (AS) model incorporates the above-mentioned data. Moreover, the seismogenic faults of Cyprus have been included into the European Database of Seismogenic Faults (EDSF, Basili et al. 2013), which is a compilation of fault sources assessed of being capable of generating earthquakes of magnitude $M_w \geq 5.5$. Crustal seismicity is computed thanks to the fault sources and is incorporated into the Fault Source and Background (FSBG) model. The top traces and planes of composite seismogenic faults for Cyprus, as collected by INGV, are mapped in Fig. 2, together with the isodepth lines of the subducting African plate. In addition to these, an extended homogenized strong motion
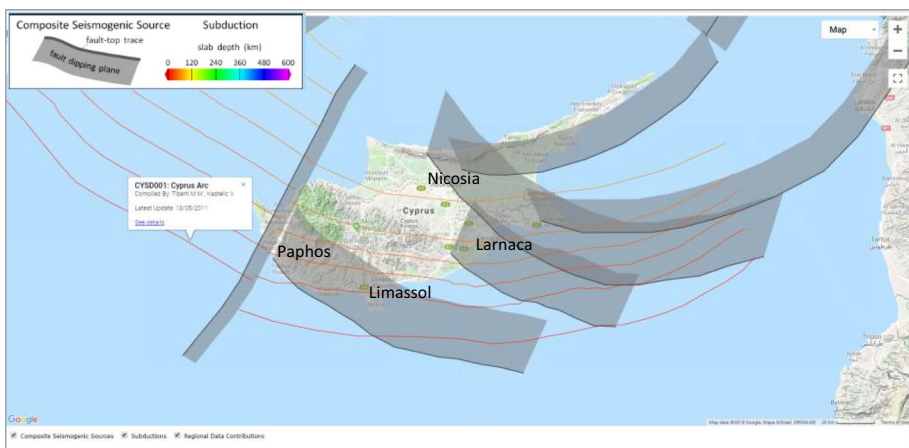
Fig. 2 Extract of the European Database of Seismogenic Faults.(Basili et al. 2013)

database (Yenier et al. 2010), with input from several existing databases, has been compiled. The SEIFA model, the third among the SHARE source models, is a kernel-smoothed model that generates earthquake rate forecasts based on fault slip and smoothed seismicity.

2.1 Probabilistic seismic hazard analysis

As first step, a classical probabilistic seismic hazard analysis (PSHA) is performed, in order to derive a hazard curve at each computation site and hazard maps, for given probability of exceedance of the intensity measure levels within the investigation time. PSHA, with all its uncertainties and complexities, is a quantitative comprehensive tool, good for design purposes, when it is necessary to associate ground motion intensities with exceedance probabilities, accounting for all possible earthquake ruptures with their return period. Strategic decisions upon the selection of the most appropriate scenario are then taken in a less arbitrary way.

The classical integration procedure as proposed by Cornell (1968) and formulated by Field et al. (2003) has been incorporated into OpenQuake platform (Pagani et al. 2014) and performed in the study herein for investigation time of 50 years. The input files for OpenQuake engine (Pagani et al. 2014) are the three *Seismic source* models of SHARE project (Giardini et al. 2013), and the *ground motion model*, as proposed by SHARE project (published in Delavaud et al. 2012). The latter associates ground motion prediction equations (GMPEs) to each tectonic region recognized in the European region, given the occurrence of an earthquake rupture.

The *logic trees* for both the above-mentioned models are essential integral component of PSHA and describe the epistemic uncertainties associated with the construction of seismic source models and the implementation of GMPEs, respectively, for different tectonic regions. The tailored source model logic tree proposed by SHARE project, used herein, is relatively simple with higher weight (50%) attributed to the area source model, 20% to FSBG (Fault-Source & Background) and 30% to SEIFA (smoothed seismicity) model. On the other hand, the *ground motion model logic tree* is more complex as it comprises a number of GMPEs differently contributing per tectonic region. The GMPEs of Table 1 with the associated weighting factors have been attributed to each tectonic regime to which Cyprus has been deemed to belong (Woessner et al. 2013).

2.1.1 Site conditions

For the definition of the *site conditions*, a simplified model based on the shear wave velocity (Vs30) map of USGS (Fig. 3) based on approximation to topographic slope (Wald and Allen 2007) has been used. Variations of Vs30 are compatible to the geological zones of the simplified geological map of Cyprus (Fig. 3, window). A more detailed geological map can be used in the future based on the data obtained from the microzonation studies conducted for most of the cities in the island (e.g. CGSD 2000).

Comparing Figs. 3 and 4a, a relative correlation exists between the USGS map for the area both for the sites closer to the coastal area but also for the ones in the municipality of Limassol. An attempt is undertaken to gather the results from all the microzonation studies in Cyprus (Paphos, Limassol, Nicosia, Famagusta) (Fig. 4a and Table 2) and compare them with the USGS map (Fig. 3). Subsequently and with the assistance of experts in the field, it is anticipated that a new map will be drawn representative of the shear wave velocities calculated at various locations in Cyprus.

Table 1 GMPEs per tectonic region of Cyprus according to SHARE models (Giardini et al. 2013)

| Tectonic regime	GMPE	Weight	Tectonic regime	GMPE	Weight
Active shallow crust	Akkar and Bommer (2010)	0.35	Subduction Interface & Inslab	Atkinson and Boore (2003)	0.20
	Cauzzi and Faccioli (2008)	0.35		Lin and Lee (2008)	0.20
	Chiou and Youngs (2008)	0.20		Youngs et al. (1997)	0.20
	Zhao et al. (2006)	0.10		Zhao et al. (2006)	0.40
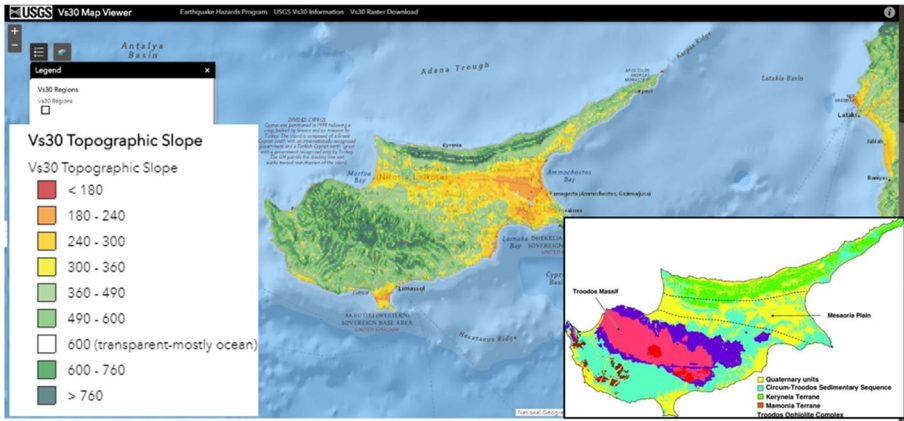
Fig. 3 Shear wave velocity map of Cyprus (USGS 2020); (window) simplified geological map of Cyprus (Cohen et al. 2012)

The study resulted to the following proposed microzonation map (Fig. 4b), which discretizes the area to three seismic zones with defined peak ground acceleration levels. These are similar to the ones adopted later on by the Cyprus Seismic Hazard map introduced in the National Annex of Eurocode 8–1.

2.1.2 Probabilistic output hazard

The information extracted from the probabilistic seismic hazard analysis is summarized in the *seismic hazard curve,* which combines the rate (or probability) of exceedance of a range of intensity levels for different ground motion parameters at a given site. This curve is composed by considering all possible earthquake ruptures included in the seismic source model, which, within the given investigation time of 50 years, exceed the ground motion parameter levels.

The curves below depict the peak ground acceleration (PGA) (Fig. 5a) and the spectral acceleration at $T=0.3$ s (Fig. 5b) with the corresponding probability of exceedance in 50 years. They have been plotted for the main cities of Cyprus for which PGA varies between 0.3 and 0.5 g and Sa varies between 0.7 and 1.0 g. It may be seen that the seismic hazard in Limassol and Paphos, in the south, south-western part of the island, is the most elevated in the island, being in the vicinity of the shallow seismic subduction zones of the Cyprus and the Hellenic Arc (Fig. 2). The PGA (Fig. 6) and SA distribution for poe$=10\%$ ($T=475y$) and poe$=2\%$ ($T=2500y$) throughout the island have been mapped in Kazantzidou et al. (2019) and are compatible to the seismic hazard map of ESHM13 (Giardini et al. 2014), with incorporation of the soil contribution. The mapped values of the seismic hazard distribution for $T=475y$ (Fig. 6a) yield higher values than the seismic zonation map of the current seismic design code (Fig. 7c) and higher values than the microzonation study of Limassol (Fig. 4b). This is explained by the different seismic catalogue that has been used for the code and for ESHM13, the input of which is implemented herein. Also, the lack of a calibrated model for the subduction zone located at the south of the island might be a factor that affected the anticipated hazard in the area and overestimates the seismic hazard in the area as predicted in by ESHM13 model.

(a)

(b)
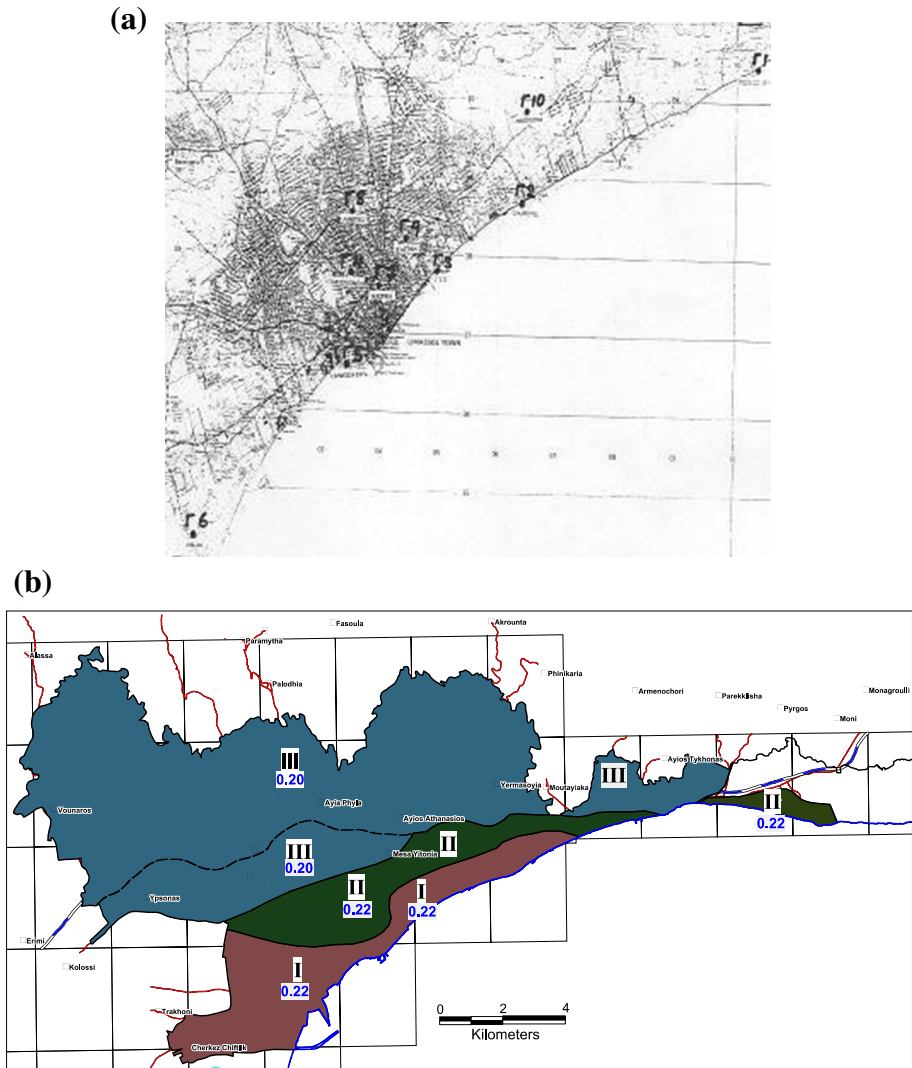
Fig. 4 **a** Location of boreholes used for Vs30 calculations in the microzonation study of Limassol (Anasta-siades et. al. 2006). **b** Proposed microzonation map of Limassol area (Anastasiades et al. 2006)

3 Event-based probabilistic seismic risk analysis

Risk analysis, by definition, is the convolution of the seismic hazard model and the vulnerability model applied over the layer of the assets (structures or population) exposed to the hazard of the area of study. For the risk estimation, herein, the event-based probabilistic analysis was implemented, as developed in OpenQuake engine (Silva et al. 2013). Compared to the classical PSHA-based risk analysis, the probabilistic, or stochastic event-based, is based on the classical principles of PSHA, yet computing relies on the compilation of synthetic catalogues of earthquake ruptures for which a ground motion field is
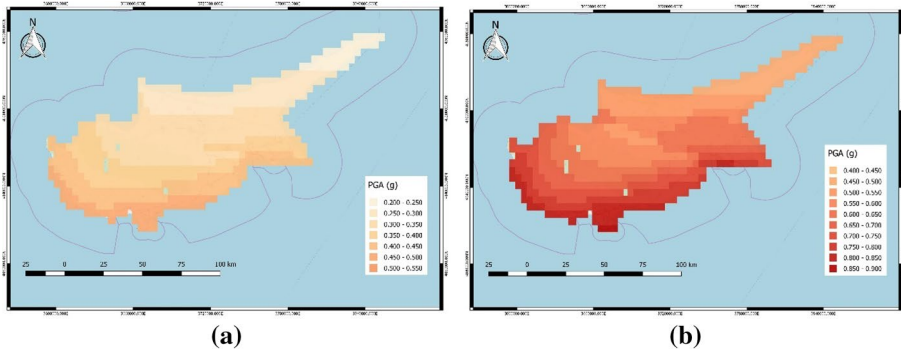
Table 2 Average Vs30 values per borehole from the microzonation study of Limassol (Anastasiades et. al. 2006)

| Borehole number	Average (Vs)	Borehole number	Average (Vs)
Γ1	500	Γ6	380
Γ2	280	Γ7	460
Γ3	320	Γ8	370
Γ4	380	Γ9	380
Γ5	300		
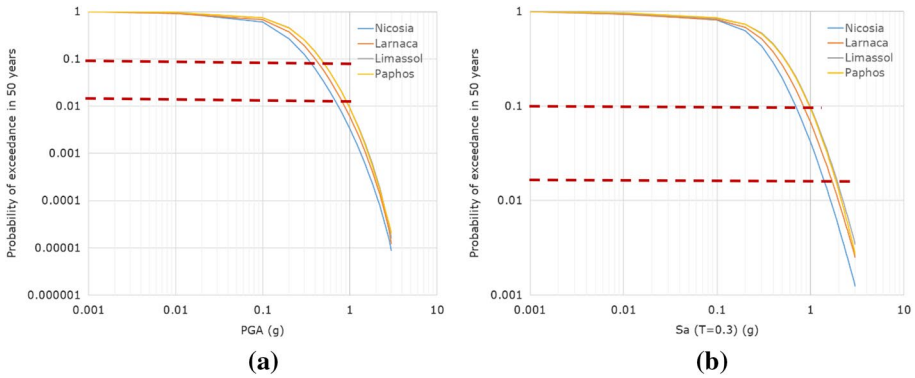
Fig. 5 Hazard curves for the main cities of Cyprus in **a** PGA and **b** Sa from PSHA

Fig. 6 PGA distribution for **a** T=475y and **b** T=2500y according to PSHA

generated. According to this, a large number of potential earthquake scenarios, together with their probability of occurrence, are to be included in the hazard computation. Compared to the classical PSHA, stochastic event-based achieves to simulate seismicity of a region in a realistic, yet randomly generated way, reflecting the actual tectonic environment, earthquake catalogue and expected events recurrence, accounting for epistemic and aleatory uncertainties of the models and hazard results. This is of particular interest for the risk/loss estimation, since all the assets overlaid by the ground motion fields contribute cumulatively to the aggregated loss curve.
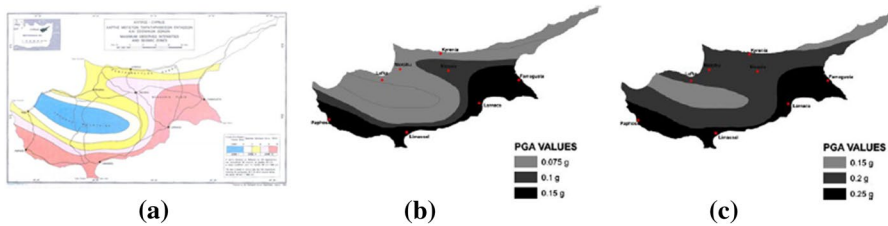
Fig. 7 Seismic design codes, according to **a** 1978 guidelines, **b** CCEAA (1992) and **c** update of 2004 (**a** from Chrysostomou 2009; **b,c** adapted from Cagnan and Tanircan 2010)

Initially, a stochastic event-based hazard analysis is conducted by inputting the *seismic source* and *ground motion models together*, as described above for the classical PSH analysis. The Earthquake Rupture Forecast calculator of the engine generates a number of all possible ruptures within the area of study for the given seismic sources and estimates associated probability of occurrence within a given time span. The Stochastic Event Set calculator, then, allows for the simulation of the number of occurrence of each rupture within a given time span with the implementation of a sampling process similar to Monte Carlo (Musson 2000). This leads to the creation of one or more stochastic sets of events (synthetic catalogues of earthquake ruptures), which simulate the seismicity in a region. For each of the events, the ground motion model with its logic tree is applied and a *ground motion field* (geographic distribution of the intensity measure of a ground motion around a rupture) is computed. Aleatory variability at inter- or intra-event basis is taken into account, while spatial correlation of intra-event residuals may be also considered. Given the computational effort the stochastic event-based analysis at national level requires, spatial correlation has been neglected herein. The set of ground motion fields is spatially combined with the exposure model and its vulnerability, and the probabilistic event-based risk calculator computes the estimated loss value per asset and per each ground motion field with the associated annual frequency of exceedance.

3.1 Exposure model

The exposure model is a crucial component of risk modelling as it contains all the information of assets (buildings and permanent population herein) exposed to given levels of hazard and "thereby subjected to potential loss" (UNISDR 2009). The source of information is of primary importance and depending on the level of detail of the study and of the expected outcome, building inventory databases can be compiled with different levels of accuracy. Part of the exposure dataset is the economic replacement value of the different building typologies, necessary information for the economic loss estimation as direct risk outcome.

3.1.1 Building stock and population

In the current study, in which the risk assessment is conducted at national level, information was obtained from the national building and population census record of 2011 and the GIS-based building database of the Department of Lands and Surveys (DLS). The DLS building inventory contains data about registered buildings with official

building permit, while the building census complemented the model with non-officially registered buildings. For the northern part of the island, data were obtained from the corresponding Census of 2006. All data were collected by the local representatives who participated in EMME project (Giardini et al. 2016), as reported in Chrysostomou et al. (2014) and was kindly provided by the authors of the latter work for the purposes of the current study. Within EMME project, a $1 \times 1 km^2$ grid was generated for the entire island, and the population and buildings registered in the inventory per district have been distributed across the grid cells, together with their registered characteristics. These include the building material, the period of construction and their number of stories.

The classification of buildings per typology has taken place following the European Building Taxonomy Classification, as defined during the RiskUE project (2003). The criteria of the classification are: (i) the material, (ii) the construction period, (iii) the design codes employed and (iv) the building height. Hence, the following typologies are available, according to Chrysostomou et al. (2014): load-bearing masonry, reinforced concrete (RC) frames for low- and mid- to high-rise buildings and further distinction of RC structures for low ductility (with no Earthquake Resistance Design—"no ERD") and moderate ductility ("ERD" buildings). The mid- to high-rise buildings have been grouped together, based on the availability of fragility curves, as explained below and the low availability of damage to the former category.

As far as the seismic design code evolution is concerned, according to Chrysostomou (2009), in the aftermath of the major Thessaloniki's earthquake in 1978, the Cypriot Commission for Earthquake Measurements was established. The first measurements were then set up in Cyprus for the protection of the population and the built environment from earthquake hazard. Furthermore, the first guidelines for the seismic design of reinforced concrete and masonry buildings were issued, as the first attempt to incorporate lateral loads in the structural design of buildings. It was only in 1992 that the Association of Civil Engineers and Architects of Cyprus (ASEAC 1992), drafted the first Cypriot Seismic design code, based on the CEB standards (CEB 1991). Its implementation was optional until 1994 when it was put in mandatory force. Until then, engineers had the option to select the implementation of any of the international codes they were familiar with. Finally, according to 2011 Regulation, Eurocodes, with their National Annexes, were introduced as obligatory standard for structural/seismic design with no other standard in parallel use since 2012. With regard to the northern part, the seismic design was enforced in 1999 with the Turkish earthquake code, updated in 2007 (TEC 2007).

The first seismic zonation map was proposed with the Guidelines of 1978, in terms of seismic intensity, being based on data of historical earthquakes. The island was divided into four isoseismic zones with intensities ranging between $I = 6$ (white) and 10 (red) (Fig. 7a). Within 1992 Code (CCEAA 1992) (Fig. 7b), the first seismic zonation in terms of peak ground acceleration was introduced with zones compatible to the former map and values ranging between 0.075 g and 0.15 g in the southern, most seismic part of the island. Lateral loads were then taken into account as the respective ratio of acceleration of gravity. In 2004, the new seismic zonation was published (Fig. 7c) and remains into force up to date. It is evident that the update was to the safe side as the design accelerations were upgraded to 0.15 g and 0.25 g, respectively, and the moderate zone was extended to a larger part of the island.

As far as the type of buildings is concerned, it has been reported (Chrysostomou et al. 2014) that the vast majority of load-bearing masonry buildings was built prior to 1975. Simple stone, most commonly sand stone, constitutes the typical material of the traditional
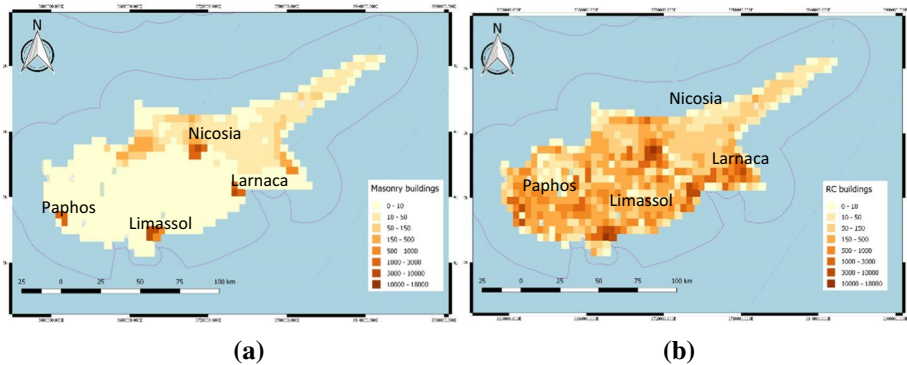
Fig. 8 Distribution of number of **a** masonry and **b** RC buildings

Cypriot architecture, especially in Nicosia and Limassol, the larger cities (Papadouris 1990). It is used along with mortar and often combined with timber elements. Moreover, mudbrick is an old material for adobe structures mainly found in rural communities in the alluvial plains. It is often protected by gypsum or mud plaster with timber wedges. However, since no detailed information is given with respect to the typology of masonry, no distinction was made between adobe and simple stone material.

Maps in Fig. 8 illustrate separately the spatial distribution of residential buildings of reinforced concrete and masonry buildings throughout the island. As expected, there is a high concentration (> 3000 buildings per grid) in the big cities (Nicosia, Paphos, Limassol, Larnaca). Masonry buildings, if not accounting for the big cities, are mostly concentrated in the northern part of the island, which, historically, has undergone the least economic development. On the other hand, RC buildings are more unevenly distributed throughout the island, and this is also encountered among buildings with and without ERD (Fig. 9); the latter being mostly concentrated in the urban centres of the island earlier developed. This observation is compatible with the trend of urban expansion during the past 40 years. The latter map of RC distribution is compatible with population distribution with higher concentrations in the four big cities.

Figure 10 demonstrates the typological distribution of residential buildings throughout the island with ratios and absolute numbers. The total number of buildings, as registered in the Census, is 326820. It is evident that low- to mid-rise RC buildings with no seismic design (ERD) is the predominant typology (57% of the building stock), accommodating the 54% of the island's population. Its counterpart with ERD is the most common typology (23%). Seventeen percente of the registered building stock is made of bearing masonry, being mainly encountered in the northern part of the island (Fig. 8a), if not accounting for the major cities. Approximately the 15% of the population lives in masonry buildings, being one of the lowest ratios in Europe, according to the exposure model developed in SERA project (Crowley et al. 2020). High-rise buildings correspond to be around the 3% of the island's building stock. It should be noted that a number of high-rise buildings have been erected in the main cities after 2011 but, considering that these are individual structures following the most modern seismic design provisions, their exclusion from the exposure model is not considered to significantly affect the overall risk outcome.
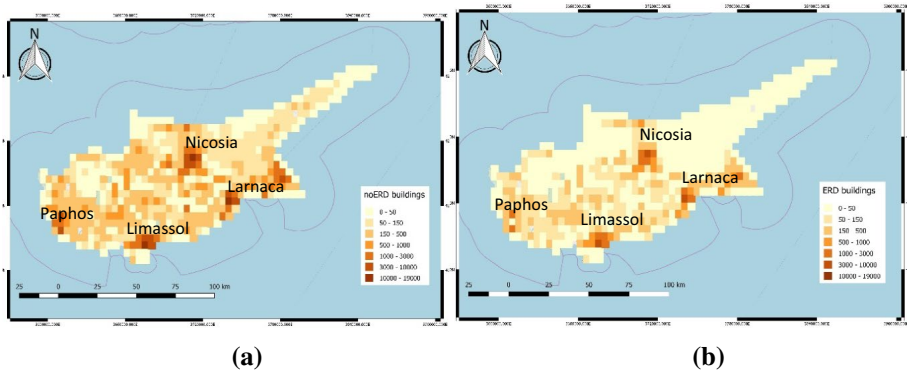
Fig. 9 Distribution of RC buildings built **a** without earthquake-resistant design (ERD) and **b** with ERD

3.1.2 Building replacement value

The replacement value, i.e. the actual cost of an asset to be currently rebuilt, is a term coming from insurance world and belongs to the exposure module of a risk study, aiming to loss assessment at economic terms. Based on empirical data and experts' solicitation, the average area per floor for residential buildings has been set for older/no ERD typologies equal to 80 and for younger ones equal to 100m^2. The replacement cost only for structural works ranges between 600 and 800 euro/m^2 with higher cost attributed to ERD high- and low-rise buildings, both corresponding to newer luxurious structures. Replacement values do not include non-structural elements. The total structural replacement value of the exposed residential assets is estimated around 32 billion euro. As discussed during the exchanges for the creation of SERA exposure model (Crowley et al. 2020), additional parameters may be taken into account, herein neglected for simplification purposes. Some of these are: differentiation per urban/rural areas, additional labour and transfer costs in remote areas, material cost due to seismicity zone.

3.2 Vulnerability and consequence modelling

Within a National Risk Assessment study, the selection of the appropriate and most representative available vulnerability model is a highly scientific and demanding process, as the assessment of the vulnerability component is crucial and a determining factor of the risk estimate. The implementation of vulnerability models derived from published local studies, when available and trustworthy, is strongly recommended. Fragility curves, analytically developed for local typologies, have incorporated a range of local material properties and construction and design practices, varying among different countries and eras, local structural detailing and reinforcement ratio, varying even for the same structural systems due to different building codes or local practices, e.g. spacing of stirrups or mortar thickness, architectural peculiarities and other characteristics determinant for buildings' seismic performance. Should empirical results be available, validating the computational fragility estimates, it is also recommended to be employed, at building capacity or final performance level.
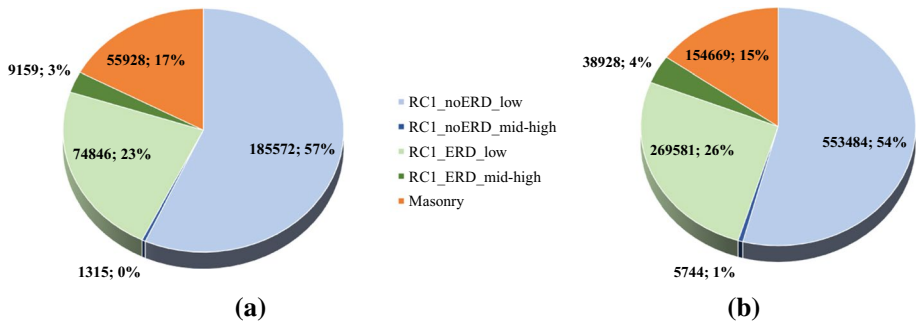
Fig. 10 Distribution of **a** building typologies and **b** population per building typology for Cyprus

In the current study, the fragility curves analytically derived by Kyriakides et al. (2015) have been used for the vulnerability simulation of reinforced concrete (RC) buildings. Fragility curves for low-rise frame buildings (for average height of 2 stories) have been generated, due to the multitude of this typology, as well as fragility curves for high-rise frame buildings (for average height of 7 stories), due to their observed vulnerability. The curves correspond to buildings without any seismic design provision ("No ERD" prior to 1992) and with ERD, according to the Cypriot Seismic design after 1992. To account for building variability within each structural typology, structural characteristics (material strength and detailing) were treated probabilistically using the Latin hypercube sampling technique. In total, 60 building models have been simulated and 420 time-history analyses were performed for seven sets of real acceleration records matched to the elastic acceleration spectrum derived for the two seismic zones of Limassol in the microzonation study of CGCD (2000).

Mid-rise buildings of 3–5 stories height have not been thoroughly examined by Kyriakides et al. (2015) due to low damage recording from previous earthquakes and limited resources. After engineering judgment, fragility curves of high-rise category, with average number of storeys equal to six, were attributed to the mid- to high-rise category of building.

As far as bearing masonry buildings are concerned, in the absence of local studies, it has been decided to make use of curves referenced in the literature of the same region, for which engineering expertise demonstrates the existence of similar typology as in Cyprus. Hence, from the GEM/OpenQuake Physical Vulnerability Database (GEM 2020b), the analytical fragility curves developed by Ahmad et al. (2011) for the Euro-mediterranean low- to mid-rise masonry buildings have been selected. The curves are derived after nonlinear static analyses of prototype 2D buildings and seismic hazard obtained from 10 natural US accelerograms and IBS-2006 rock acceleration spectra. Uncertainties in lateral stiffness, strength and damage limit states are taken into account through Monte Carlo simulations.

Important issue when different vulnerability models are employed is the compatibility and harmonization of damage states as well as intensity measures. With regard to the latter, all fragility curves selected are derived against peak ground acceleration. Damage states implemented herein follow the 4-grade scaling of HAZUS (FEMA 2003) with qualitative generic description for all building typologies. However, the qualitative approach requires an agreement on the empirical interpretation and computational equivalence of each damage state along the capacity curve. Hence, below (Table 3) are enlisted the Damage States

for RC buildings, as adopted by Kyriakides et al. (2015) following EN1998 (CEN 2004) performance thresholds, and corresponding inter-storey drift limits for masonry buildings, as employed by Ahmad et al. (2011) according to UPAV (for SYNER-G project; VCE 2011) or DBELA methodology (Calvi 1999).

The final risk estimate is based on vulnerability curves, functions that describe a total loss ratio for each level of intensity measure.These imply the adoption of a consequence (or damage ratio) model to be combined with the fragility curves. The consequence model expresses the ratio of cost of repair with respect to the cost of replacement for each damage state. This is usually constructed based on damage information claimed by householders in financial terms following a damaging earthquake when requesting financial aid. These data were not easily available with the current resources for Cyprus, and thus, published models by Kappos et al. (2006), based on the Greek reality, have been adopted considering no major discrepancies due to the similarities of structural typologies: {RC: 5%(S), 20%(M), 45%(E), 80%(C); M: 12%(S), 30%(M), 55%(E), 85%(C)}.

In Fig. 11a, vulnerability curves for all aggregated building typologies are illustrated and respective loss ratios per damage state in Fig. 11b. Considering the small discrepancies among the damage ratios of RC and masonry typologies, the curves' level can be representative of the vulnerability of the typologies, with masonry being the most vulnerable, followed by RC no-ERD low-rise typologies. Interestingly, among the no-ERD typologies, the low-rise buildings are slightly more vulnerable than the high-rise ones, what can be explained by the realization that higher levels of redistribution take place in high-rise buildings and higher compressive forces on columns increase their capacity. Additionally, in practice high-rise buildings tend to have more elaborated construction detailing and average material properties, which has not been modelled at this phase. Among ERD buildings, low-rise exhibit less vulnerable behaviour.

3.3 Risk and economic loss outcome

First outcome of the probabilistic risk analysis (here stochastic event-based) is the derivation of the mean loss exceedance curve (i.e. list of aggregated losses for respective probabilities of being exceeded) for the entire portfolio of assets (Kazantzidou-Firtinidou et al. 2019). This is constructed for all assets, considering all possible paths of the hazard logic trees and for the cumulative impact that may be exceeded of all earthquakes that might occur during the investigation time.


(a)

(b)
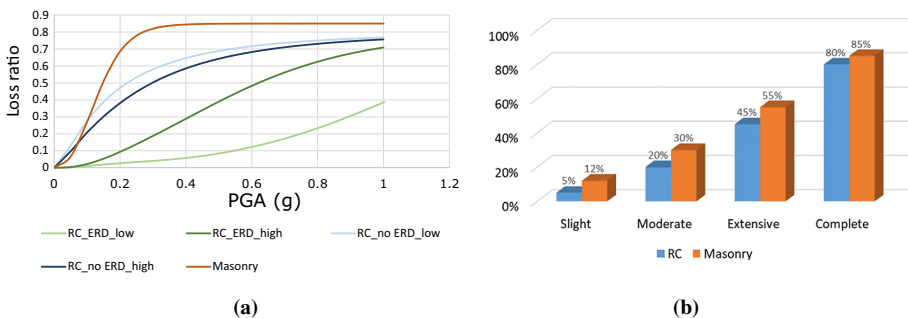
Fig. 11 **a** Loss curves for aggregated building typologies considered and **b** loss ratios for RC and masonry typologies

Hence, the expected aggregated mean loss with $T=475$ years (or 10% poe in 50y) is 3.46 billion euro, what corresponds to 10.8% mean loss ratio and the 14.1% of Cyprus island GDP (gross domestic product). The expected aggregated mean loss is 6.3 billion euro with $T=2500$ years (or 2% poe in 50y), what corresponds to 19.8% mean loss ratio or 25.6% of Cyprus island GDP. The mean loss ratio is calculated with normalization of the aggregated loss over the total replacement value of the entire building portfolio (~32 billion euro). Losses account only for structural cost and do not consider losses due to non-structural or content damage. It should be noted that the aggregated losses are calculated over a sum of events that may occur throughout the investigation time for a given probability.

As for the spatial distribution of losses, the probabilistic loss maps below (Fig. 12) illustrate the aggregated average losses per grid for $T=475y$ (left) and $T=2500y$ (right). The spatial distribution does not change significantly for the two return periods, and the highest loss is concentrated in the urban areas with the highest exposure (Fig. 8). It is noted that Limassol (in South) presents the highest expected loss, while the affected area of Nicosia is more extended as opposed to Paphos and Larnaca. For $T=475y$, mean aggregated losses expected to reach 550 M in certain urban locations, while this metric might reach 750 M for $T=2500y$.

The estimated average annual loss (AAL) that corresponds to the risk investigation time ($t=50$ years) is equal to 116 million euro, approximately the 0.50% of the island's GDP. Moreover, the *average annual loss ratio (AALR)* for the residential building portfolio is estimated equal to 0.36%. AALR is computed as the fraction of the average annual loss with the total building replacement value (only structural cost) and is a representative normalized metric of loss, often employed for comparison purposes. Comparison with risk results of GEM Foundation (Silva et al. 2018), which concludes to total (sum of residential, commercial and industrial) AAL equal to 295 million euro and AALR equal to 0.14%, is not straightforward as the current study takes into account only structural replacement cost and loss while GEM's includes structural, non-structural and contents cost. It should be also noted that GEM has not included the northern part of the island and differences may be also attributed to the use of different fragility curves, what proves the importance of the structural component. Spatial distribution of AAL and ALLR is qualitatively well compatible although the current study employs a larger resolution. Table 4 lists the AAL and AALR as well as the
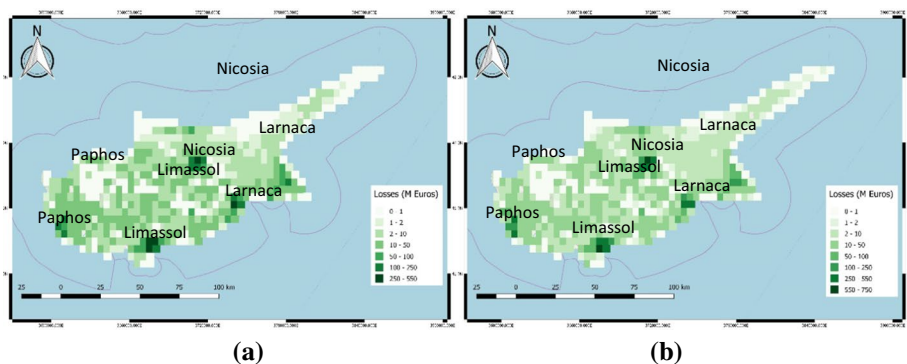
Fig. 12 Loss map (in million euro) for **a** 10% poe in 50 years ($T=475$ years) and **b** for 2% poe in 50 years ($T=2500$ years)

Table 3 Damage scale and limit states

| Damage states (per FEMA 2003)	Overall damage description (per FEMA 2003)	RC limit states (per EN1998)	Masonry limit states (per UPAV, Ahmad et al. 2011)
Slight	Negligible-to-slight damage No structural damage, slight non-structural damage	$\theta_{columns} \geq \theta y$	LS1
Moderate	Slight structural damage Moderate non-structural damage	$\theta_{columns} \geq 3/4 * \theta u$	LS2
Extensive	Moderate structural damage. Heavy non-structural damage	$\theta_{columns} \geq \theta u$ and $V_{columns} \geq Vu$	LS3
Complete	Heavy-to-very-heavy structural damage Very-heavy non-structural damage Total or near-total collapse	All columns $\theta_{columns} \geq \theta u$ or maxD $\geq 4\%$	LS4

exposed population for the entire island and for the major cities. Figure 13 illustrates the spatial distribution of AAL and AALR throughout the island. The largest cities concentrate the highest AAL, as expected, while AALR is increased in a larger extent, especially in the southern part of the island. Uncertainties upon the assumption of the grid cells per city, including a larger are than the urban part of the metropolitan cities, should be taken into account. It is interesting that Nicosia's exposed population is higher than Limassol's for significantly lower average annual loss and loss ratio, what is explained by the high population density of Cyprus capital (Nicosia), the higher number of replacement value of the exposed assets in Limassol and increased seismic hazard within the same return period. Furthermore, ALLR is also significantly higher in Limassol, what explains better the combined vulnerability and hazard that buildings in Limassol experience, independently of their population and replacement value.

Figure 14 illustrates the disaggregation of the total average annual loss and average annual loss ratio per structural typology. The latter has been computed over the total replacement value assumed per typology. From both figures, it is evident that masonry and RC-no-ERD low-to-mid-rise buildings contribute the most to the total average annual loss being the most vulnerable typologies. This is even more evident when studying the loss in terms of loss ratio, accounting for the replacement value of the exposed assets of given typologies. Observing the latter normalized results, masonry buildings have the highest loss ratio, which is compatible with their being the most vulnerable typology (Fig. 11). As a matter of fact, no-ERD low-to-mid-rise buildings correspond also to the largest building population (Fig. 10), what places them on top of the overall loss contribution ranking, while masonry buildings, although of low exposure (Fig. 10), contribute largely to the total structural loss due to their high vulnerability.

Compatible to the above-mentioned average annual results are the aggregated conclusions for the two studied return periods ($T=475y$, $T=2500y$). More precisely, the

Table 4 Average annual loss (in euro) and corresponding exposed population

	Total	Nicosia	Larnaca	Limassol	Paphos
AAL	116 M	13.0 M	8.7 M	23.6 M	9.0 M
AALR	0.36%	0.31%	0.44%	0.69%	0.63%
Population	1,022,406	143,558	37,771	127,629	40,012

(a) (b)
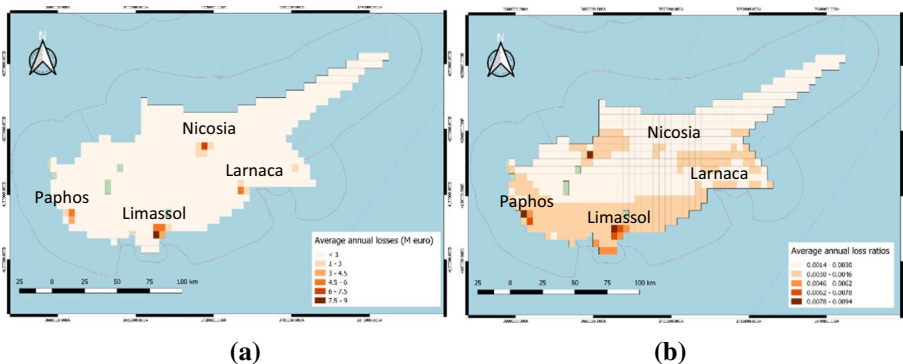
Fig. 13 a. Average annual loss and b. average annual loss ratio
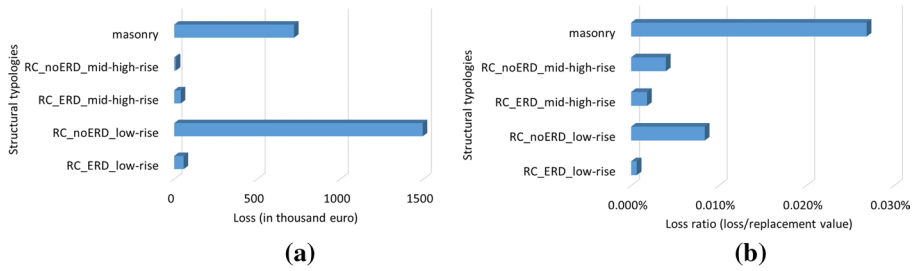
Fig. 14 Disaggregation of **a** average annual loss (AAL) and **b** AAL ratio per structural typology

aggregated economic impact mentioned above is expected to be attributed to masonry damage within a range of 15 to 18% and 70 to 75% to RC-no-ERD low-to-mid-rise buildings respectively. Interestingly, most recent RC ERD buildings are expected to contribute less (3.5% against 7.8% for $T = 475y$) in the case of $T = 2500y$. This can be explained by the fact that new constructions, mainly in the area of Limassol, are less affected by the seismic faults with higher return period, according to the seismic catalogue considered. On the other hand, no conclusions can be drawn with regard to correlation of particular typologies with hazard distribution at national scale, considering smooth hazard reduction from SW to NE and typologies distribution of Figs. 8 and 9.

4 Scenario-based analysis

Disaster risk management tends to opt for scenario-based analysis, which gives more specific and understandable results for operational purposes, while also providing more comprehensive outcomes and allows for further elaborations that are necessary for capacity building and training purposes. Often, selection varies among the most probable, the worst-case and historical scenarios. The latter with empirical observations allow for cross-validation of analytical results and are often employed for calibration of the input models of probabilistic analysis. Within NRA, for every hazard, three (3) scenarios are identified and selected, compatible with each other for compilation of overall risk matrix. These are (a) the worst-case scenario—plausible with upper risk limit/level, (b) expected scenario—the scenario to be prepared for, and (c) best case/mild scenario—plausible with lower risk limit.

In the current study, two seismic scenarios have been selected to be presented, one being the expected scenario (with $T = 475$-year return period aggregate loss) and one representative of the worst-case scenario (with $T = 2500y$ aggregate loss). The selection of the earthquake ruptures has been randomly made among all different realizations of the existing stochastic catalogue that are able to generate aggregated losses with given return periods. The scenarios have been selected based on the probabilities of occurrence of losses being selected in correspondence with the design earthquake and the most credible earthquake scenarios. The stochastic catalogue has been generated by OQ by collecting all possible ruptures produced by the set of seismic sources (SHARE model input) over a given fixed time span. The GMPE that was decided to be implemented was that of Akkar and Bommer (2010), following the recommendation of Cagnan and Tanircan (2010). Each scenario was

performed for a number of 1000 ground motion fields (for different ruptures within the fault).

In Fig. 15, the fault lines and surface for the two scenarios are projected on the earth's surface on the island of Cyprus. The fault geometry and characteristics and the rupture magnitude of the selected events are also marked. The expected scenario ($T = 475$y) is simulated by a fault that lies southern of Limassol with significantly high moment magnitude (Mw7.7), while the worst-case scenario (with $T = 2500$y) has significant length, runs inland along the western shore of the island, while its moment magnitude is lower (Mw6.9) [5]. It is, thus, noted that the probability of occurrence has been employed as unique criterion for the scenarios selection, what does not necessarily imply that the "worst case", with the highest return period, yields the most adverse results. As a matter of fact, the highest values of PGA for both scenarios do not differ significantly, due to similar characteristics of seismogenic faults, other than their length (Fig. 15). Faults of important length, as proved in Fig. 16, are able to affect a significantly extended area. Hence, although absolute PGA values converge, the PGA distribution and the zones affected by different ground acceleration values differ significantly. The exposed assets that lie within the different PGA zones will be determinant for the final risk and loss outcome.

4.1 Damage and economic loss

Scenario damage and risk assessment have been performed for the selected earthquake rupture scenarios, taking into account epistemic and aleatory uncertainties. Damage statistics exported include mean values and standard deviation for the number of buildings that are expected to suffer the four different damage states for which the fragility curves have been defined. In the collapse maps of Kazantzidou-Firtinidou et al. (2019), spatial distribution of buildings estimated to experience damage at the state of collapse or nearly collapse
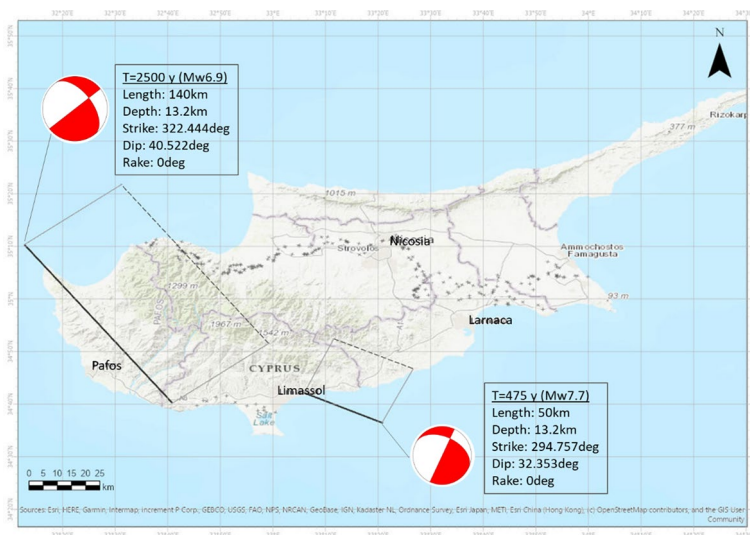
Fig. 15 Seismological characteristics of two seismic scenarios analysed
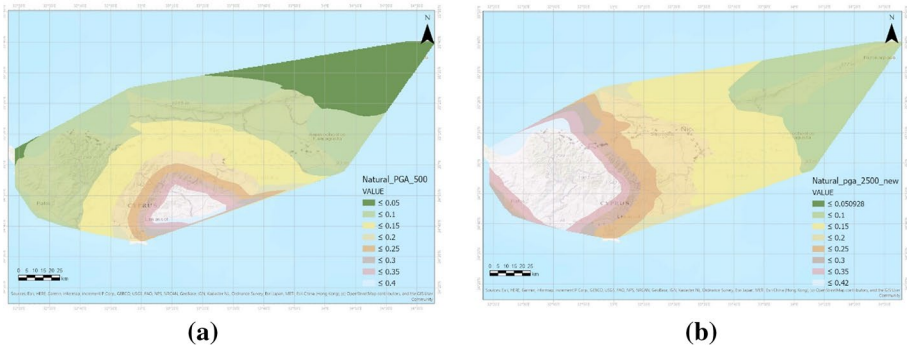
Fig. 16 PGA distribution for scenario **a** $T=475y$ and **b** $T=2500y$

was illustrated. For Scenario $T=475y$, collapses are mainly concentrated to the southern and central parts of the island, where Limassol, Larnaca and Nicosia are also located. On the other hand, collapses for $T=2500y$ scenario are mostly located to the westernmost side of Cyprus, with Limassol being the only urban area. As discussed, the spatial distribution of hazard values in correlation to the building stock and its characteristics determine the final damage statistics.

Figure 17a demonstrates the number of buildings that suffer from different damage states for the two analysed seismic scenarios. It is interesting to notice that the ~83,000 buildings (25.64%) and ~106,000 (32.52%) (% of the total building stock) for the $T=475y$ and the $T=2500y$ scenario are expected to reach the "Complete" damage state, respectively. On the other hand, ~130,000 (40.07%) and 105,000 (32.19%) buildings, respectively, are expected to present no damage. In addition, the chart of Fig. 17b depicts the ratio of collapsed buildings per structural typology, clearly demonstrating the most vulnerable typologies. It is evident, therefore, that for both scenarios for the masonry and the no-ERD low- to-mid-rise typologies, more than 30% of their stock is expected to present damage at the level of collapse. For the case of scenario $T=2500y$, this ratio exceeds even 40%, what is explained by the spatial distribution of PGA, affecting large zones and most importantly urban areas.

The disaggregation of the damage outcome per structural typology (Fig. 18) provides observations for further analysis and indications for potential targeted interventions. The presentation of results with the ratio of damaged buildings per total stock of each structural typology provides more representative results of the typological performance for each scenario. For the $T=475y$ and $T=2500y$ scenarios, in addition to the previous observations, a significant ratio of more than 20% of no-ERD high-rise buildings presents extensive damage at both scenarios. On the other hand, among the ERD buildings, high-rise buildings are expected to suffer more significant damage, as 8–10% are estimated to be extensively damaged. The latter is compatible to the fragility curves of Fig. 9.

Figure 19 depicts the distribution of the aggregated economic loss per grid for the $T=475y$ (left) and $T=2500y$ (right) scenarios. Considering the vicinity of the fault for $T=475y$ to Limassol (Fig. 15) and the high exposure value, Limassol and its surroundings is the most heavily affected area. Considering the scenario for $T=2500y$, the affected areas are shifted to the western part of the island, compatible to the faults trace location. Although the number of collapsed buildings may not change significantly,
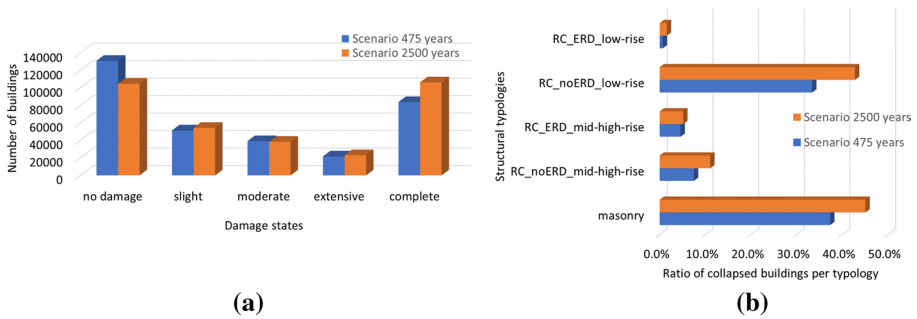
Fig. 17 a Distribution of number of buildings per damage state and **b** ratio of collapsed buildings ("complete") over total number of buildings per typology for the two scenarios

more important levels of damage are observed to a larger amount of structures and to more extended zones, what is also compatible to the distribution of loss. Among the big cities, the highest economic loss is expected in Limassol for both scenarios (Table 5), due to both the high concentrated damage and the high exposed replacement value. The area that corresponds to each city has been attributed to the corresponding grid cells with the best possible approximation. Monetary loss is quite significant across the island for both scenarios, since a large number of buildings are expected to suffer from damage and significant structural loss. The total amount is significantly higher than the outcome of stochastic event-based for the respective return periods ($T = 475y$, $T = 2500y$), considering that the mean loss for the scenarios is averaged out across the different simulations performed within the event, while in the event-based calculations there is a single inter-event mean and sigma value associated with losses of a specific return period.

At this point, it would be necessary to mention the possibility and usefulness of an integrated risk analysis, accounting for both physical and social vulnerabilities. The latter, being a complex and multidimensional concept, is able to assist to identify those characteristics and experiences of population that enable them to respond and recover from natural hazards (Cutter et al. 2003). Practically, it obtains a (comparative) measure through the variations of socio-economic variables that may alternate impacts of seismic hazard on population and state's economy. The integration of these variables, by means of calibrated indices, into the physical modules, is able to modify the final risk impact and is part of the so-called integrated risk analysis (Burton et al. 2014). Social indices, implemented in the final risk outcome, are able to decrease or aggravate aggregated or distributed loss values. This has not been implemented in the current study as it implies deep elaboration of local socio-economic data.

4.2 Human loss

For the seismic scenarios, risk is estimated also in terms of human loss, casualties and displaced population. Civil Defence and Healthcare authorities, at national level and as decentralized administrations, could make use of the estimated figures in order to build capacities and allocate necessary budget. The order of magnitude of the estimated figures is to be employed, and the outcome of a range of scenarios can be additionally analysed.
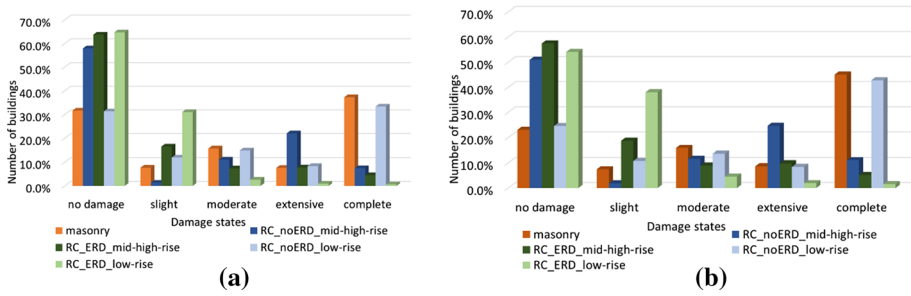
Fig. 18 Disaggregation of damaged buildings per damage state and structural typology for seismic scenario with **a** $T = 475y$ and with **b** $T = 2500y$
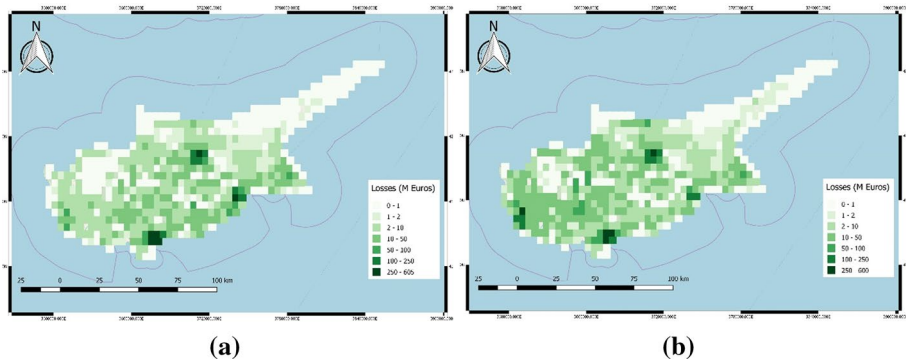
Fig. 19 Loss map for seismic scenario with **a** $T = 475$ years and **b** $T = 2500$ years (right)

Table 5 Monetary loss estimated for the four major cities, for the two analysed scenarios

	Total	Nicosia	Larnaca	Limassol	Paphos
Scenario $T = 475y$	7.7B	1.1B	530 M	1.6B	150 M
Scenario $T = 2500$ y	9.5B	1.1B	363 M	1.3B	645 M

For the seismic scenarios, risk in terms of human loss has been also estimated in order to obtain a number of affected population to be elaborated as order of magnitude for disaster management purposes. This estimate is valuable for preparedness of the Civil Defence and municipalities for healthcare capacities, short- and long-term accommodation, emergency response and relevant budget allocation.

4.2.1 Casualties

For the estimation of non-fatal casualties, or injuries in need of a greater degree of medical care and in need of transition to healthcare facilities, the model adopted was proposed by HAZUS (1999) for indoor casualties and it has been applied only for Injury Severity 2 (Injuries requiring a greater degree of medical care). Hence, the casualty event tree described by HAZUS (1999) has been trimmed for estimation of Severity 2

Table 6 Casualty rates per severity level and damage state (DG)

	Slight (%)	Moderate (%)	Extensive (%)	Complete (%)
Reinforced concrete	0.0	0.03	0.10	1.0
Masonry	0.0	0.10	0.20	2.0

injuries, to which all the branching probabilities (all four fragility curves) contribute with different weights for the main building typologies (Table 6):

$$P_{\text{Sev.2}} = \left[P(\text{ds}_{\_S}) * P_{\text{Sev,2-}S} + P(\text{ds}_{\_M}) * P_{\text{Sev,2-}M} + P(\text{ds}_{\_E}) * P_{\text{Sev,2-}E} + P(\text{ds}_{\_C}) * P_{\text{Sev,2\_}C} \right] * M_2$$

$P(\text{ds}_{\_i})$ with $i=S$ (slight), M (moderate), E (extensive), C (complete) is the probability for each damage state (fragility curves). $P_{\text{Sev,2-}i}$ with $i=$S,M,E,C is the probability of injuries per damage state in ratios, as proposed by HAZUS (1999).

The M2 coefficient, to account for occupancy rates at residential and non-residential buildings, differentiates daytime and night-time. It is taken equal to 0.49 for daytime and 0.70 at night-time, assuming 80% residential buildings and 20% non-residential. Occupancy rates of 40% for residential building in daytime and 75% for non-residential are assumed. Similarly, 75% for residential and 40% for non-residential buildings are assumed for night-time. Further investigation could be made based on actual statistical data, what has been though out of the scope of the present study.

The expected number of occupants injured per Severity 2 or in fatal state ($\text{EN}_{\text{occupants}}$) is a product of the number of occupants per asset at the time of earthquake (daytime, night-time) ($N_{\text{occupants}}$) and their probability of being injured ($P_{\text{Sev,2}}$), computed as vulnerability curves in loss human ratio terms. The population included in the input file refers to the total registered population per asset, as given by the 2011 Census and elaborated by Chrysostomou et al. (2014).

$$\text{EN}_{\text{occupants\_Sev,i}} = N_{\text{occupants}} * P_{\text{Sev,2}}$$

For modelling of fatalities, the model of Coburn and Spence (2002) has been adopted with the values for the parameters as proposed by Spence for Thessaloniki case study (Greece) within LESSLOS project (Spence 2007). This model enables the straight correlation of casualties with the vulnerability of the buildings, other than their use. Fatalities have been separately estimated for daytime and night-time, considering 80% of residential buildings and 20% of non-residential. Only the 1% of the fragility curves of the "complete" damage state are considered to contribute to the fatalities estimation, as following the model adopted herein; given "complete" state only the 1% is expected to collapse. The base model is:

$$K_S = \left[M_1 \cdot M_2 \cdot M_3 \cdot \left(M_4 + M_5 \cdot (1 - M_4) \right) \right]$$

where M_1: the occupancy rate per building block (number of people/m^2 of building area). Here it is adopted equal to 0.025, mean proposed value for Thessaloniki (thus 40 m^2 per inhabitant), for simplification equal for all typologies. M_2: a coefficient that depends on the use of the building at the time the earthquake strikes, equal to 0.49 for day and 0.7 for night use. M_3: ratio of inhabitants trapped in the building due to collapse, given "Collapse" of the "Complete" state. This parameter is based on empirical data and an average value of 0.18 is adopted for the 475 years scenario and 0.26 for the 2500 years scenario.

As proposed for the case of Thessaloniki, the 0.01 of the buildings in "complete" state are expected to completely collapse. M_4: the coefficient that correlates collapse with fatalities (dead or unsavable), taken for RC buildings equal to 0.4 and for masonry equal to 0.1, based on empirical casualty data and building collapse mechanisms. Similarly, the 0.01 of the buildings in "complete" state is expected to completely collapse. M_5: stands for the mortality due to collapses, taken as 0.7 for RC buildings and 0.45 for masonry buildings, again based on empirical statistical data.

In Table 7, the numbers of fatalities and injuries (severity 2) have been enlisted for the major cities, as a range between the day and night estimates. Although emergency management at municipality level requires risk assessment at higher resolution level and highly accounts for operational needs, the estimates enlisted herein provide an overview of the human impact of the two analysed scenarios throughout the island. Moreover, the ratios of the affected population with respect to the exposed population in the same cell grids are also marked. Although the absolute numbers are more useful for disaster management and preparedness purposes, these relative figures provide a more representative picture of the extent each city is affected by each seismic event, acknowledging all uncertainties involved. It is noted that following the selected model, fatalities correspond only to completely collapsed buildings, while other fatalities have been neglected. The aggregated figures of casualties at national level, exceeding the summation of the major cities, indicate that affected population is well dispersed throughout the island, compatible to the damage and population distribution.

As far as the 475-year loss scenario is concerned, triggered by the activation of a WNW-ESE fault, dipping NNE, in the vicinity of Limassol, it leads to 1 fatality, for day or night scenario and few hundreds of injuries in Limassol city and its surroundings. The 2500-year loss scenario, with a 140-m-long NW–SE fault dipping NE, located towards the western part of the island, affects less Limassol, yet high numbers are also encountered in this area due to the population and buildings density. Paphos, is the most affected city for this scenario, being in the vicinity of the causative fault, with several dozens of injuries. Nicosia, with a high population density, presents injuries, ranging between 80 and 250 people for both scenarios, while no fatalities are estimated. Finally, Larnaca seems to be more affected by the 475-year scenario with 25–60 injuries. For the entire island, both scenarios yield expected injuries in the range of 700–1700 and a low total number of fatalities, no more than 6 people (Table 7).

Table 7 Casualties per scenario and major cities

Cities	Injuries				Fatalities	
	475 years		2500 years		475 years	2500 years
	People	Ratio (%)	People	Ratio (%)	People	People
Nicosia	80–200	0.06–0.14	100–240	0.07–0.16	0	0
Larnaca	25–60	0.07–0.16	10–25	0.03–0.07	0	0
Limassol	310–700	0.24–0.54	210–500	0.17–0.40	1	0–1
Paphos	3–10	0.01–0.02	60–155	0.16–0.40	0	0–1
Total	730–1500	0.07–0.15	870–1770	0.09–0.17	2–3	4–6

4.2.2 Displaced population

Earthquakes can cause loss of function or habitability of buildings, as described by the damage grades classification. The estimation of the affected number of population that would need to be displaced provides useful figures (order of magnitude) to stakeholders for anticipation of post-disaster provisions and/or evacuation planning. In the current study, it has been decided to estimate the population that would require to be displaced at long-term basis. According to the shelter model of HAZUS (1999), only residents of buildings estimated to suffer extensive and complete damage are expected to be evacuated and temporarily sheltered for a time period of few weeks up to two months (Quarantelli 1982).

$$\#DP_L = \left\{ p\left[ds_{\_E}\right] + p\left[ds_C\right] \right\} \cdot \text{Population}$$

Furthermore, in order to make a more realistic approach of the actual population that would evacuate and eventually seek public sheltering, HAZUS (1999) suggests several reduction coefficients to be applied upon the above-estimated numbers, with weight factors based mainly on US reality (ethnic, income, ownership, age considerations). In the current study, these weight coefficients have been omitted but reference is made to the need for a more thorough study based on the social vulnerability of the area and its differential distribution, in the principles of the aforementioned integrated risk analysis. The latter could lead to calibration of customized reduction factors, based on socio-economic indices (age, education, income, ethnicity, etc.), access to infrastructure, ratio of damage buildings in the area, house ownership and other dimensions able to affect the willingness or need of people to seek state's assistance.

Hence, for the estimation of an order of magnitude of evacuees in need of public temporary shelter, for which the civil protection authorities need to anticipate with procurement of material, empirical data documented in Gountromichou et al. (2017) and Kazantzidou-Firtinidou et al. (2018), as part of PACES Project, has been employed. With further experts input for Cyprus and considering the Cypriot mentality and family bonds, the possibility of ships to be used for population sheltering and the large amount of touristic lodges to be employed after safety inspection, the 50% of the estimated displaced population is expected to be in need of public sheltering in tents or other portable structures (as discussed in Kazantzidou-Firtinidou et al. 2021).

For the two analysed scenarios, national capacities should be built for a range of displaced population between 93 and 110 thousands, while optimization of storage allocation throughout the island would better be made according to the national risk map of Fig. 12, for T = 475y, accounting for a number of seismic events.

5 Conclusions

The seismic risk has been estimated at national level for the island of Cyprus, as part of the National Risk Assessment submitted to DG ECHO. A probabilistic methodology for hazard and risk assessment has been implemented, leading to the selection of seismic scenarios of 10% and 2% probability of occurrence, being compatible to the expected and worst-case scenario, respectively.

The seismic hazard, based on the European seismic hazard model of SHARE (Giardini et al. 2013) project, has been first computed with classical probabilistic seismic hazard analysis, providing expected acceleration values significantly higher than the design ones

(for 10% poe in 50 years). The input hazard is deemed to be determinant for the loss estimate. Hazard curves and maps extracted may be useful to decision-makers, such as urban planners and civil defence authorities for issuing regulations based on hazard distribution.

Stochastic event-based risk analysis, implementing the seismic catalogue as registered in SHARE project, the exposure and vulnerability models provided by local studies (Chrysostomou et al. 2014; Kyriakides et al. 2015), yields the expected aggregated monetary loss estimate for given probabilities and the average annual structural monetary loss for residential buildings. The latter is equal to 116 million euro with 0.16% being the loss ratio, estimated against the replacement value for structural works of the residential building stock of the island. The aggregated mean loss with $T = 475$ years is estimated equal to 3.46 billion euro, while for $T = 2500$ years the respective estimate is 6.3 billion euro. Acknowledging all uncertainties a national scale analysis may imply, making also reference to the large standard deviations the inter-event loss averaging is accompanied by, these outcomes can yet provide a reasonable order of magnitude of cumulative estimated losses, especially in relatively low return periods, and can be proven a viable tool in the hands of decision stakeholders.

Limassol is the city with the highest expected average annual loss and loss ratio, although the affected population is lower than Nicosia, being the capital of Cyprus Republic. This is explained, by the high replacement value of Limassol's building stock, as well as the significant damage it is expected to suffer due to its seismotectonic region. Masonry buildings, mainly located in the main cities and North island, and low- to mid-rise buildings with no seismic design, unevenly distributed throughout the island are the typologies that mainly contribute to the total monetary loss. Seismic design was only imposed in the Republic of Cyprus in 1992, and thus, more than 70% of the Cypriot building stock was erected without homogenized seismic design regulations.

Two seismic scenarios have been selected, the first is one among those of the stochastic catalogue that may lead to losses with probability of occurrence 10% in 50 years ($T = 475$y) and the second one to losses with probability of occurrence 2% in 50 years ($T = 2500$y). Both scenarios are expected to affect the entire island due to their significant length and magnitude, with maximum PGA equal to 0.4 g. Spatial distribution of ground motion and damage is compatible to the location of the earthquake ruptures. Interesting observations have been made upon the typological contribution to the overall damage and loss aftermath. For both scenarios, 80–100,000 buildings are expected to reach the level of collapse, with the majority being masonry and low-to-mid-rise buildings with no seismic design, while a small, yet not insignificant ratio of ERD is expected to suffer from extensive to complete damage. For both scenarios, the aggregated monetary loss, reaching 7.7 billion for the $T = 475$ years scenario and 9.5 billion for the $T = 2500$ years scenario is also documented, together with loss distribution throughout the island.

Scenario-based analysis allowed also for the assessment of loss at human terms, direct metric for affected population and mortality and indirect for socio-economic impact. Hence, injuries and fatalities have been estimated with the use of casualty models available in the literature (HAZUS 1999; Coburn and Spence 2002). It should be noted that consequence models for human loss are highly dependent on the local conditions, such as collapse mechanisms of most prone to collapse structures, cultural and other characteristics that determine need and willingness to seek public accommodation. For future studies, it is strongly recommended to base this result in localized research. For both scenarios, expected injuries vary between 700 and 1700 people, while no more than 6 fatalities for the worst-case scenario are estimated for the entire island. Limassol is again most highly affected, due to its vicinity to the faults, high population and building exposure. Displaced

population that will seek temporary sheltering is estimated at national level and reaches 100,000 people for both scenarios. Values for human loss estimates are again tackled with the accuracy of the order of magnitude, but they can be of outermost importance for resources and capacities allocation at preparedness phase.

Modern disaster risk management recommendations foster the implementation of risk-informed data for the development of strategies and the adoption of measurements tailored to the scientifically revealed needs. The submission of national risk assessment every two years to the European Commission allows for the improvement of risk understanding at local and EU level, as well as the involvement of additional stakeholders, reinforcing the importance of risk-driven decisions. Capacity building and management planning at preparedness and response phase tend to be supported by risk outcomes, while mitigation and prevention measures, such as anticipation of seismic strengthening budget and establishment of catastrophe insurance premiums, have been proven to be based on risk results for different portfolios. Implementation of scenario risk assessments, at different dimensions with a common scale established among different hazards, allows for comparative conclusion of the contribution of different hazards to the risk map of the country and thus supports prioritization of actions.

Concluding, it is highlighted that the current work was prepared with the scope to fulfil the obligation for submitting a National risk Assessment to the European Commission, separately studied for the main hazards of Cyprus. It was based on available data, publicly or following special request, and published scientific methodologies. It is thus noted that no update of the study was performed to include any recent developments (e.g. the new ESHM20 that replaces the former ESHM13 model); thus, the results do not necessarily reflect outcomes supported by state-of-the-art models and hypotheses. Moreover, the validations of loss estimates are deemed difficult due to the lack of comprehensive data as well as events of the studied magnitude. In a future work, the compilation of a database with historical information (seismological, structural, impact, etc.) from events of the twentieth century is anticipated, with the cooperation with governmental agencies owning the data. This will allow the validation and calibration of the models employed, further enriched by new studies in the European hazard and risk science.

Data availability Not applicable.

Code availability Not applicable.

Declarations

Conflict of interest The author declares that they have no conflict of interest.

References

Ahmad N, Crowley H, Pinho R (2011) Analytical Fragility Functions for Reinforced Concrete and Masonry Buildings and Buildings Aggregates of EuroMediterranean Regions – UPAV methodology. Internal Report, Syner-G Project 2009/2012. Euro-Mediterranean Regions (Greece, Italy, Turkey)

Akkar S, Bommer J (2010) Empirical equations for the prediction of PGA, PGV, and spectral accelerations in Europe, the Mediterranean Region, and the Middle East. Seismol Res Lett 81(2):195–206

Atkinson GM, Boore DM (2003) Empirical ground-motion relations for subduction-zone earthquakes and theirapplication to Cascadia and other regions. Bullet Seismol Soc Am 93:1703–1729

Ambraseys NN (1965) The seismic history of Cyprus. Reven Union Intern Secours Geneva 3:25–48

Ambraseys NN (1992) Reappraisal of the seismicity in Cyprus (1894–1991). Boll Geofis Teor Eds Appl 34:41–80

Anastasiades A, Pitilakis KA, Apessou M, Apostolides P, Kallioglou P, Tika TH, Michaelides P, Petrides G, (2006) Seismic response of soil formations in Limassol. 5th Hellenic conference of geotechnical and environmental engineering, Technical Chamber of Greece, Xanthi

ASEAC (1992) Seismic Code for Reinforced Concrete Structures in Cyprus, Cyprus Civil Engineers and Architects Association, Committee for Earthquake Engineering

Basili R, Kastelic V, Demircioglu M B, Garcia Moreno D, Nemser E S, Petricca P, Sboras S P, Besana-Ost-man G M, Cabral J, Camelbeeck T, Caputo R, Danciu L, Domac H, Fonseca J, García-Mayordomo J, Giardini D, Glavatovic B, Gulen L, Ince Y, Pavlides S, Sesetyan K, Tarabusi G, Tiberti M M, Utkucu M, Valensise G, Vanneste K, Vilanova S, Wössner J (2013). The European Database of Seismogenic Faults (EDSF) compiled in the framework of the Project SHARE. http://diss.rm.ingv.it/share-edsf/, doi: https://doi.org/10.6092/INGV.IT-SHARE-EDSF. http://diss.rm.ingv.it/share-edsf/. Accessed 29 Nov 2020

Burton C G, Khazai B, Silva V (2014). Social vulnerability and Integrated risk assessment within the Global Earthquake Model. Tenth U.S. National conference on earthquake engineering: frontiers of earthquake engineering, Anchorage, Alaska, USA.

Cagnan Z, Tanircan GB (2010) Seismic hazard assessment for Cyprus. J Seismol 14:225–246. https://doi.org/10.1007/s10950-009-9163-1

Calvi GM (1999) A displacement-based approach for vulnerability evaluation of classes of buildings. J Earthq Eng 3:411–348

Cauzzi C, Faccioli E (2008) Broadband (0.05 to 20 s) prediction of displacement response spectra based on worldwide digital records. J Seismol 12:453–475

CCDD (2016) 2nd Report on the National Risk Assessment of the Republic of Cyprus, Cyprus Civil Defence Department Ministry of Interior, Republic of Cyprus

CCEAA (1992) Seismic code for reinforced concrete structures in Cyprus. Committee for Earthquake Engineering, Cyprus Civil Engineers and Architects Association, Cyprus

CEB (1991) CEB-FIB model Code 1990—Final draft. Bulletins no 203/204/205. Comite Euro-international du Beton, Lausanne

CEN (2004) Eurcode 8, Design of structures for earthquake resistance-part 1: general rules, seismic actions and rules for buildings, EN 1998–1:2004. Comite Europeen de formalisation, Brussels

CGSD (2000) Microzonation study of the city of Lemesos in Cyprus. Cyprus Geological and Survey Department, Republic of Cyprus

CGSD (2017) Significant recent earthquake (1900-today), Cyprus Geological Survey Department. http://www.moa.gov.cy/moa/gsd/gsd.nsf/All/16C98663E655EFF6C22583C40046E788?OpenDocument). Accessed 29 Nov 2020

Chiou BS-J, Youngs RR (2008) An NGA model for the average horizontal component of peak ground motion and response spectra. Earthq Spectra 24:173–216

Chrysostomou (2009) Seismic Protection of Cyprus. 16th concrete conference TEE, ETEK, 21–23 October 2009, Pafos, Cyprus (in Greek)

Chrysostomou Ch, Kyriakides N, Cagnan Z (2014) Scenario-based seismic risk assessment for the Cyprus region. Proceedings of 2nd European conference on earthquake engineering and seismology, Istanbul, Turkey

Coburn A, Spence R (2002) Earthquake protection, 2nd edn. Wiley, Chichester, England

Cohen D, Rutherford N, Morisseau E, Zissimos A (2012) Geochemical patterns in the soils of Cyprus. Sci Total Environ 420:250–262

Cornell CA (1968) Engineering seismic risk analysis. Bull Seismol Soc Am 58:1583–1606

Crowley H, Despotaki V, Rodrigues D, Silva V, Costa C, Toma-Danila D, Riga E, Karatzetzou A, Fotopou-lou S, Sousa L, Ozcebe S, Gamba P, Dabbeek J, Romão X, Pereira X, Castro JM, Daniell J, Veliu BH, Adam C, Deyanova M, Ademovic N, Atalic J, Bessason B, Shendova V, Tiganescu A, Toma-Danila D,

Zugic Z, Akkar S, Hancilar U, Exposure Contributors (2020) European exposure model data repository (Version 0.9) [Data set]. Zenodo. https://doi.org/10.5281/zenodo.4062044

Cutter SL, Boruff BJ, Shirley WL (2003) Social vulnerability to environmental hazards. Soc Sci Q 84(2):242–261

Delavaud E et al (2012) Towards a ground-motion logic tree for probabilistic seismic hazard assessment in Europe. J Seismolog 16:451–473

EC (2010) Risk Assessment and Mapping Guidelines for Disaster Management. Commission Staff Working Paper, SEC (2010) 1626 final

ECORYS & Fraunhofer (2018) Peer review Cyprus 2018. 2018–2019 Programme for peer reviews in the framework of EU cooperation on civil protection and disaster risk management

Erdik M, Sestyan K, Demircioglu M, Tuzun C, Giardini D, Gulen L, Akkar S, Zare M (2012). Assessment of seismic hazard in the Middle East and Caucasus: EMME (Earthquake Model of Middle East) project. Proceedings of 15th World conference on earthquake engineering, Lisbon, Portugal

FEMA (2003) HAZUS-MH MR4. Technical Manual—Multi-hazard Loss Estimation Methodology – Earthquake Model. Federal Emergency Management Agency, Washington D.C., 2003

Field EH, Jordan TH, Cornell CA (2003) OpenSHA—A developing community-modeling environment for seismic hazard analysis. Seismol Res Lett 74:406–419

Galanopoulos A, Delibasis N (1965) The seismic activity in the Cyprus area. Prakt Akad Athenon 40:387–405

GEM (2020a) Global Earthquake Model Foundation. https://www.globalquakemodel.org/. Accessed 29 Nov 2020

GEM (2020b). GEM/OpenQuake Physical Vulnerability Database , Global Earthquake Model Foundation. https://platform.openquake.org/vulnerability/list Accessed 29 Nov 2020

Giardini D et al. (2013). Seismic Hazard Harmonization in Europe (SHARE): Online Data Resource - http://www.efehr.org/en/Documentation/specific-hazard-models/europe/hazard-computation-input/. Accessed 29 Nov 2020

Giardini D, Woessner J, Danciu L (2014) Mapping Europe's seismic hazard. Eos 95(29):261–262

Giardini D, Danciu L, Erdik M, Sesetyan K, Demircioglu M, Akkar S, Gülen L and Zare M (2016) Seismic hazard map of the middle ea0000000st. https://doi.org/10.12686/a1

Gountromichou C, Kazantzidou-Firtinidou D, Goretti A, Kyriakides N (2017) Deliverable B2d—Seismic scenarios focused on the operational preparedness and planning, PACES Project

HAZUS (1999) Earthquake loss estimation methodology – technical and user manuals. Federal Emergency Management Agency, Washington D.C.

ISO (2018) ISO 31000:2018, Risk management—Guidelines. International Organization for Standards, Geneva, Switzerland

ISO (2019) ISO31010:2019, Risk management—Risk assessment techniques. International Organization for Standards, Geneva, Switzerland

Kalogeras I, Stavrakakis G, Solomi K (1999) The October 9, 1996 earthquake in Cyprus: seismological, macroseismic and strong motion data. Ann Geofis 42:85–97

Kappos A, Panagopoulos G, Panagiotopoulos C, Penelis G (2006) A hybrid method for the vulnerability assessment of R/C and URM buildings, Bull Earthquake Eng 4:391–413

Kazantzidou-Firtinidou D, Gountromichou C, Kyriakides K, Liassides P, Hadjigeorgiou K (2018) Seismic Risk Assessment as a basic tool for emergency planning: "PACES" EU project. Disaster Manag Human Health Risk V WIT Trans Built Environ 173:43–54

Kazantzidou-Firtinidou D, Kyriakides N, Chrysostomou C (2019) Earthquake Risk Assessment for Cyprus. 2nd international conference on natural hazard and infrastructure, 23–26 June, Chania

Kazantzidou-Firtinidou D, Sakkas G, Papathanasiou C, Eftychidis G (2021) Risk-based methodological approach for planning for emergency sheltering due to earthquake disasters. Special Issue "Technology Advances and Support for Security Practitioners" of the "Security Informatics and Law Enforcement". ISBN: 978-3-030-69460-9

Kyriakides N, Chrysostomou Ch, Tantele E, Votsis R (2015) Framework for the derivation of analytical fragility curves and life cycle cost analysis for non-seismically designed buildings. Soil Dyn Earthq Eng 78:116–126

Lin P-S, Lee C-T (2008) ground-motion attenuation relationships for subduction-zone earthquakes in Northeastern Taiwan. Bullet Seismol Soc Am 98(1):220–240

Musson R (2000) The use of Monte Carlo simulations for seismic hazard assessment in the U.K. Annali in Geofisica 43:1

Pagani M, Monelli D, Weatherill G, Danciu L, Crowley H, Silva V, Henshaw P, Butler L, Nastasi M, Panzeri L, Simionato M, Vigano D (2014) OpenQuake engine: an open hazard (and risk) software for the global earthquake model. Seismol Res Lett 85(3):1–13

Papadouris G (1990). Building materials in the traditional architecture of Cyprus. Association of Cypriot Archaeologists, Repubic of Cyprus (in Greek)

Papazachos BC, Papaioannou CA (1999) Lithospheric boundaries and plate motions in the Cyprus area. Tectonophysics 308:193–204

Quarantelli EL (1982) Sheltering and housing after major community disasters: case studies and general conclusions. Disaster Research Center, Ohio State University, Columbus, OH

Sesetyan K, Demircioglu M, Rovida A, Stucchi M (2011) SHARE-CET, the SHARE earthquake catalogue for Central and Eastern Turkey complementing the SHARE European Eartquake Catalogue (SHEEC). Catalogue available at: https://www.emidius.eu/SHEEC/

Silva V, Crowley H, Pagani M, Monelli D, Pinho R (2013) Development of the OpenQuake engine, the Global Earthquake Model's open-source software for seismic risk assessment. Nat Hazards 72(3):1409–1427

Silva V, Amo-Oduro D, Calderon A, Dabbeek J, Despotaki V, Martins L, Rao A, Simionato M, Viganò D, Yepes C, Acevedo A, Horspool N, Crowley H, Jaiswal K, Journeay M, Pittore M (2018) Global Earthquake Model (GEM) Seismic Risk Map (version 2018.1). https://doi.org/10.13117/GEM-GLOBAL-SEISMIC-RISK-MAP-2018.1

Spence R (ed) (2007) Earthquake Disaster scenario prediction and Loss modelling for Urban areas, LESS-LOS Report, IUSS Press, Pavia

Stucchi et al (2013) The SHARE European earthquake catalogue (SHEEC) 1000–1899. J Seismolog 17:523–544

TEC (2007) Specification for structures to be built in disaster areas. Ministry of Public Works and Settlement Government of Republic of Turkey

UNISDR (2009) Terminology of Disaster Risk Reduction. United Nations Office for Disaster Risk Reduction, Geneva, Switzerland

UNDRR (2019) Global Assessment Report on Disaster Risk Reduction. United Nations Office for Disaster Risk Reduction, Geneva, Switzerland

UNISDR (2015) Sendai Framework for Disaster Risk Reduction 2015–2030. United Nations Office for Disaster Risk Reduction, Geneva, Switzerland

UNISDR (2017) National Disaster Risk Assessment, Governance System, Methodologies and Use of Results. United Nations Office for Disaster Risk reduction, Geneva, Switzerland

USGS (2020) Global Slope - Based Vs30 Map, Unites States Geological Survey Department. https://earthquake.usgs.gov/data/vs30/ Accessed 29 Nov 2020.

VCE—Vienna Consulting Engineers (2011) D7.1-Functional Fragility Curve Archive, SYNER-G project Systemic Seismic Vulnerability and Risk Analysis for Buildings, Lifeline Networks and Infrastructures Safety Gain

Wald DJ, Allen TI (2007) Topographic slope as a proxy for seismic site conditions and amplification. Bull Seismol Soc Am 97(5):1379–1395

Wdowinski S, BenAvraham Z, Arvidsson R, Ekström G (2006) Seismotectonics of the Cyprian Arc. Geophys J Int 164:176–181

Woessner J, Danciu L, Kästli P, Monelli D (2013) Databases of seismogenic zones, Mmax, earthquake activity rates, ground motion attenuation relations and associated logic trees. SHARE Project Deliverable D6.6. http://www.efehr.org/en/Documentation/specific-hazard-models/europe/hazard-computation-input/ Accessed 29 Nov 2020.

Yenier E, Sandikkaya MA, Akkar S (2010) SHARE D4.1—Updated strong-ground motion database

Youngs RR, Chiou S-J, Silva WJ, Humphrey JR (1997) Strong ground motion attenuation relationships for subduction zone earthquakes. Seismol Res Lett 68(1):58–73

Zhao JX, Zhang J, Asano A, Ohno Y, Oouchi T, Takahashi T, Ogawa H, Irikura K, Thio HK, Somerville PG, Fukushima Y, Fukushima Y (2006) Attenuation relations of strong ground motion in Japan using site classification based on predominant period. Bull Seism Soc Am 96(3):898–913